

NASA Technical Memorandum 86294

RESIDUAL MECHANICAL PROPERTIES OF Ti-6AL-4V
AFTER SIMULATED SPACE SHUTTLE REENTRY

RONALD K. CLARK
JALALIAH UNNAM

AUGUST 1984



National Aeronautics and
Space Administration

Langley Research Center
Hampton, Virginia 23665

RESIDUAL MECHANICAL PROPERTIES OF

Ti-6Al-4V AFTER SIMULATED SPACE SHUTTLE REENTRY

Ronald K. Clark
NASA Langley Research Center
Hampton, VA

Jalaiah Unnam
Vigyan Research Assoc., Inc.
Hampton, VA

Abstract

Oxidation and embrittlement are concerns in use of titanium foils for shielding advanced space transportation system vehicles during Earth reentry. Ti-6Al-4V in 0.003 in. and 0.035 in. thicknesses were exposed to multiple cycles of simulated space transportation system ascent-reentry conditions at temperatures ranging from 1000°F to 1200°F. Residual mechanical tests and metallurgical analyses were made on the specimens after exposure. Results show that tensile elongation is the mechanical property most affected by the reentry environment. Results are presented to show a comparison of residual properties of foil specimens from static oxidation exposure and cyclic oxidation exposure.

Introduction

A number of concepts involving metallic heat shields have been studied for radiatively cooled thermal protection systems (TPS) for advanced reusable space transportation system vehicles and hypersonic aircraft (refs. 1, 2, and 3). One such metallic heat shield concept called "multiwall" consists of discrete tiles or panels which have multiple layers of dimpled and flat foils bonded together at the crest of the dimpled sheets. Multiwall panels are designed for the thermal and stress conditions characteristic of their service environment. Multiwall panels for verification of design have been fabricated using titanium-6 aluminum-4 vanadium (Ti-6Al-4V) in foil gages of 1.5 to 6 mil in thickness. The projected maximum use temperature for Ti-6Al-4V TPS panels is 1000°F.

Ti-6Al-4V is a lean-beta-alpha composition alloy. Aluminum which appears as substitutional atoms exists in the alloy as an alpha stabilizer. Vanadium which also appears as substitutional atoms exists as a beta stabilizer. Common interstitial elements found in titanium are carbon, hydrogen, nitrogen, and oxygen. Carbon, nitrogen, and oxygen are alpha stabilizers while hydrogen is a beta stabilizer. Alpha-beta alloys are heat treated at temperatures in the alpha-beta field (1675°F to 1850°F) to obtain a fine mixture of alpha and beta phases which yields maximum ductility consistent with the strength level. In the heat treatment of alpha-beta titanium alloys the behavior of the beta phase is of primary concern. The amount and composition of the beta phase affects its transformation characteristics and, thus, governs the hardening and softening of the alloy. The size and shape of the alpha grains has only a minor influence on tensile properties (ref. 4).

An intermediate ordered phase of Ti_3Al forms in this alloy at temperatures less than 1300°F. Although there is an apparent similarity in microstructure of Ti_3Al and the alpha phase, the intermediate phase has a strong influence on several mechanical properties (ref. 5). Data showing the influence of cooling through the Ti_3Al phase field (1675°F to 1850°F) on the properties of an alpha phase alloy indicate that slow cooling rates result in significantly higher ultimate and yield strengths (ref. 5). The elongation and modulus increase slightly with slow cooling through the temperature region where the Ti_3Al phase forms.

When heat treating, time is needed for the atoms to diffuse and adjust to the temperature at which the alloy is exposed. Metastable beta can form in alpha-beta alloys which contain sufficient amounts of beta-stabilizing elements to retain the beta phase at room temperature on rapid cooling from the alpha-beta or beta phase fields. Subsequent exposure to temperatures below the alpha-beta field results in changes in the microstructure as the amount of alpha phase increases through transformation of the beta phase (ref. 5).

In addition to microstructural changes that may occur in titanium with exposure to elevated temperature, exposure to an oxygen containing environment produces a thin surface oxide of TiO_2 with an oxygen enriched region underneath. The formation of the oxide scale represents a loss in material thickness which may be significant for thin foil material. The oxygen enriched layer is highly alpha-stabilized (alpha case) and is less ductile than the non-contaminated alloy (refs. 6, 7, and 8). Thus changes in mechanical properties of Ti-6Al-4V with exposure to high temperature oxidizing environments result from changes in microstructure, including the possible formation of intermetallic compounds, and/or contamination by

oxygen. The mechanical property most severely affected by high temperature oxidation is ductility.

This paper presents results from an experimental program to determine the effects of simulated TPS service conditions on the mechanical and metallurgical characteristics of Ti-6Al-4V in 0.003 in. and 0.035 in. thicknesses and to determine the feasibility of using static oxidation tests to simulate space transportation system (STS) ascent-reentry conditions. Cyclic exposure of specimens were conducted at peak temperatures of 1000° and 1100°F to simulate STS ascent-reentry conditions for 100 missions. Static oxidation exposures of specimens were conducted at temperatures ranging from 1000° to 1200°F. The duration of the static exposures were determined from kinetic considerations so that the oxygen pickup would equal the oxygen pickup during a cyclic exposure with a peak temperature equal to the static oxidation temperature (ref. 9). Residual mechanical and metallurgical analyses were made on the specimens after exposure. Results from the cyclic tests are compared to the static test results.

Procedure

Materials and Specimens

Tensile specimens were fabricated from 0.003 in. foil and 0.035 in. sheet Ti-6Al-4V in a mill annealed condition. Table I gives the chemical analysis of the foil and sheet material. The chemical analysis data for the foil material were determined by wet-chemical analysis of a sample of the material and the chemical analysis data for the sheet material were obtained from the certification of test report provided by the vendor. Figure 1 shows two specimen designs utilized in the program. The specimen design details were dictated by two considerations. The first was the size of the facility that was used to do the simulated STS exposure and the desire to have the load transfer points outside the hot zone of the facility. The specimen design shown in figure 1(a) met that consideration. The second consideration was the need for specimens with a uniform exposure history throughout the gage length. The shorter gage-length specimen in

Table I.- Chemical Analysis of Ti-6Al-4V

Element	0.035 in. sheet	0.003 in. foil
Al	6.3	5.74
V	3.9	4.18
Fe	0.13	0.15
C	0.026	0.02
O	0.16	0.233
H	0.013	0.013
N	0.021	0.039
Y		<0.0005
OE*		<0.10
OET**		0.40
Ti	BAL	BAL

*Other elements.

**Other elements total.

figure 1(b) met that consideration. Figure 1(a) type specimens were used for the simulated STS exposures. Most specimens were then transformed by machining to figure 1(b) type specimens using that portion of the longer specimen that experienced uniform exposure.

Specimens were cleaned and heat treated using procedures and conditions analogous to those used in fabricating Ti-6Al-4V multiwall panels (refs. 10 and 11). Table II gives the cleaning procedure for all specimens. Specimens were heat treated in argon using the heat-treatment cycle shown in figure 2. This heat-treat cycle is similar to the cycle utilized in the diffusion bonding (LID) process for fabricating Ti-6Al-4V multiwall panels (refs. 10, 11, and 12).

Apparatus and Exposure Conditions - Cyclic Tests

Simulated STS exposures of tensile specimens were conducted in the NASA Langley Research Center Multiparameter Test System (ref. 13). This facility provides programmed variation of specimen load (stress), temperature, and air pressure. Air which is bled into the system to regulate pressure is filtered and dried to two parts water per million parts of air. Each chamber accommodates up to six specimens simultaneously. Load is controlled independently for each specimen. Figure 3 shows the cyclic stress, temperature, and pressure variations that were input for one series of tests with a maximum temperature of 1000°F. These data were derived from a review of Space Shuttle ascent and reentry trajectories.

Tensile specimens from foil and sheet material were exposed to 100 cycles of ascent-reentry conditions with and without stress with a maximum temperature of 1000°F (STS 1000). Foil gage tensile specimens were also exposed to 100 cycles of ascent-reentry conditions with and without stress with a maximum temperature of 1100°F (STS 1100). Three specimens were exposed at each condition. One specimen from each group was used for metallurgical analysis and two were used in mechanical tests. The only difference in test conditions for the STS 1100 exposures and the test conditions for the STS 1000 exposures is that the temperature rise at the start of reentry (fig. 3) continues to 1100°F where it is held constant for about 6 minutes. Specimens were cooled by forced or natural convection as required to achieve the indicated cooling rate.

Apparatus and Exposure Conditions - Static Tests

Tensile specimens of foil material were exposed to static oxidation at atmospheric pressure in laboratory air at temperatures ranging from 1000°F to 1200°F. Foil gage tensile specimens were also exposed to static oxidation at 7 torr pressure at 1100°F and 1200°F. The atmospheric pressure tests were performed in a laboratory air furnace and the low pressure tests were performed in the multiparameter tests system. Three specimens were exposed at each condition. One specimen from each group was used in metallurgical analyses and two were used in residual mechanical property tests.

The exposure times for the static oxidation tests were estimated such that the total weight gain by the specimen during static exposure would equal the total weight gain by a specimen undergoing cyclic oxidation (STS exposures) where the peak temperature of the cycle equals the static

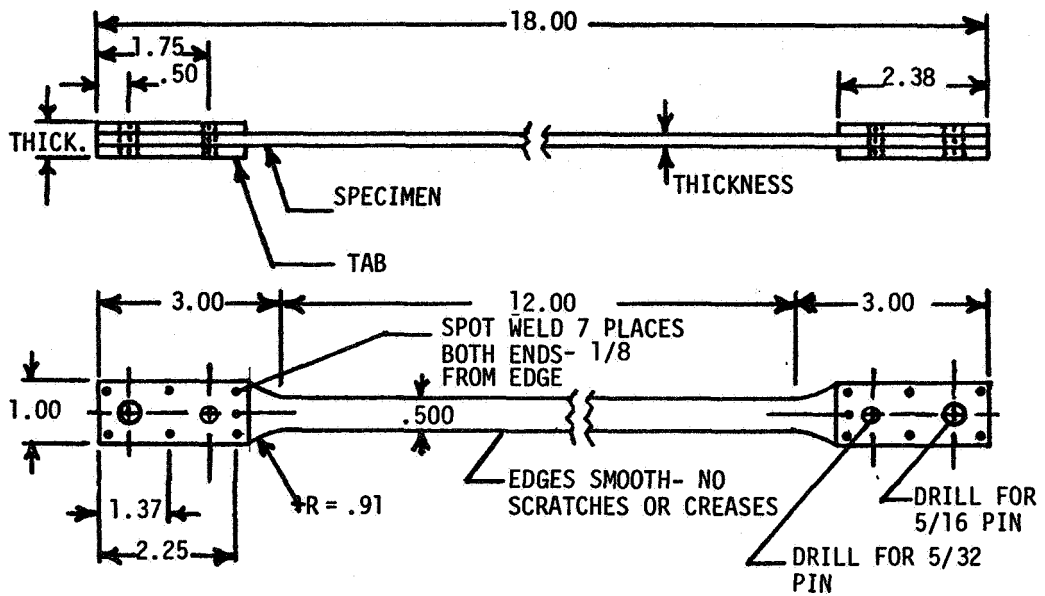


Figure 1(a)- Specimen design for simulated STS exposure of Ti-6Al-4V in the NASA Langley Multiparameter Facility (dimensions in inches).

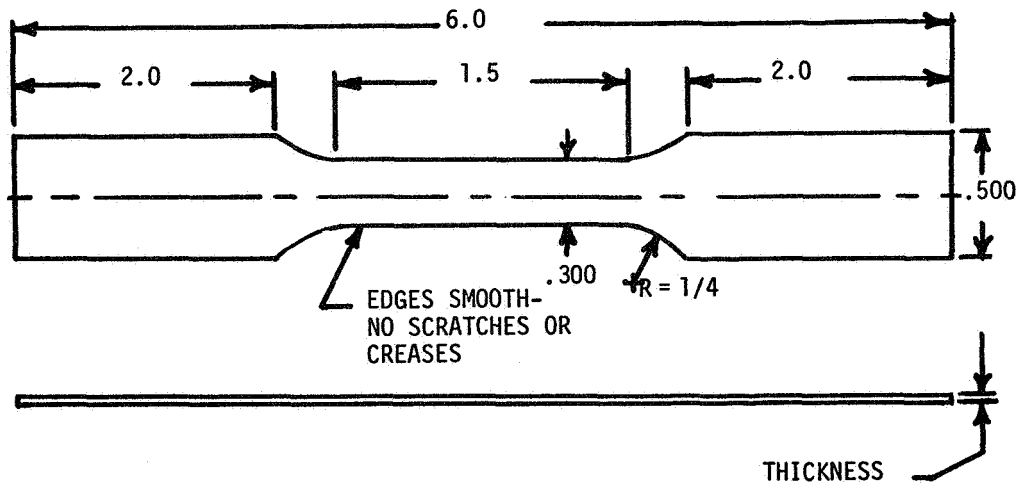


Figure 1(b)- Subsize tensile specimen design for residual mechanical tests (dimensions in inches).

Table II.- Cleaning Procedure for Titanium Specimens

Step	Process
1	Vapor degrease
2	Hot NaOH Bath - 160°F, 15 minutes
3	Water rinse - deionized water
4	Pickle - 50% HNO ₃ , 3% HF, for 2 minutes
5	Water rinse - deionized water
6	Ethyl alcohol rinse
7	Forced air dry

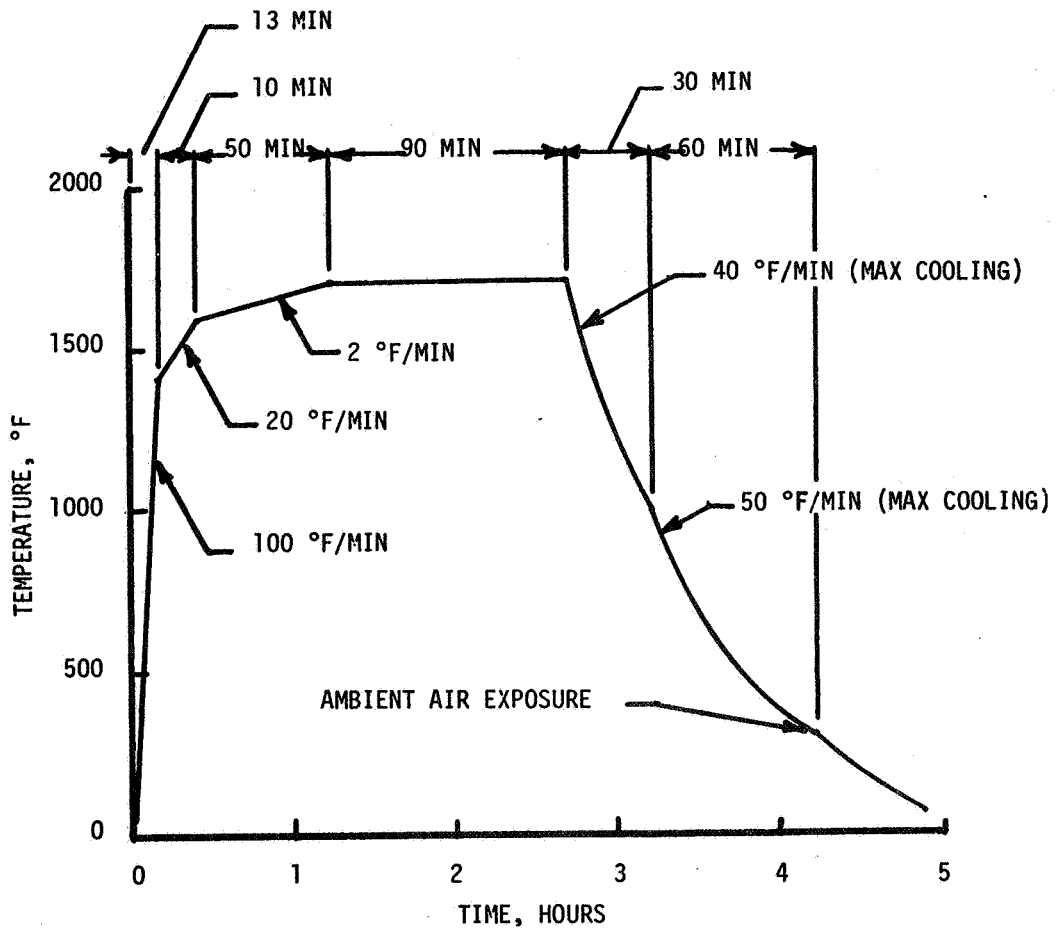


Figure 2- Nominal heat treatment cycle for diffusion bonding (LID) of titanium structures.

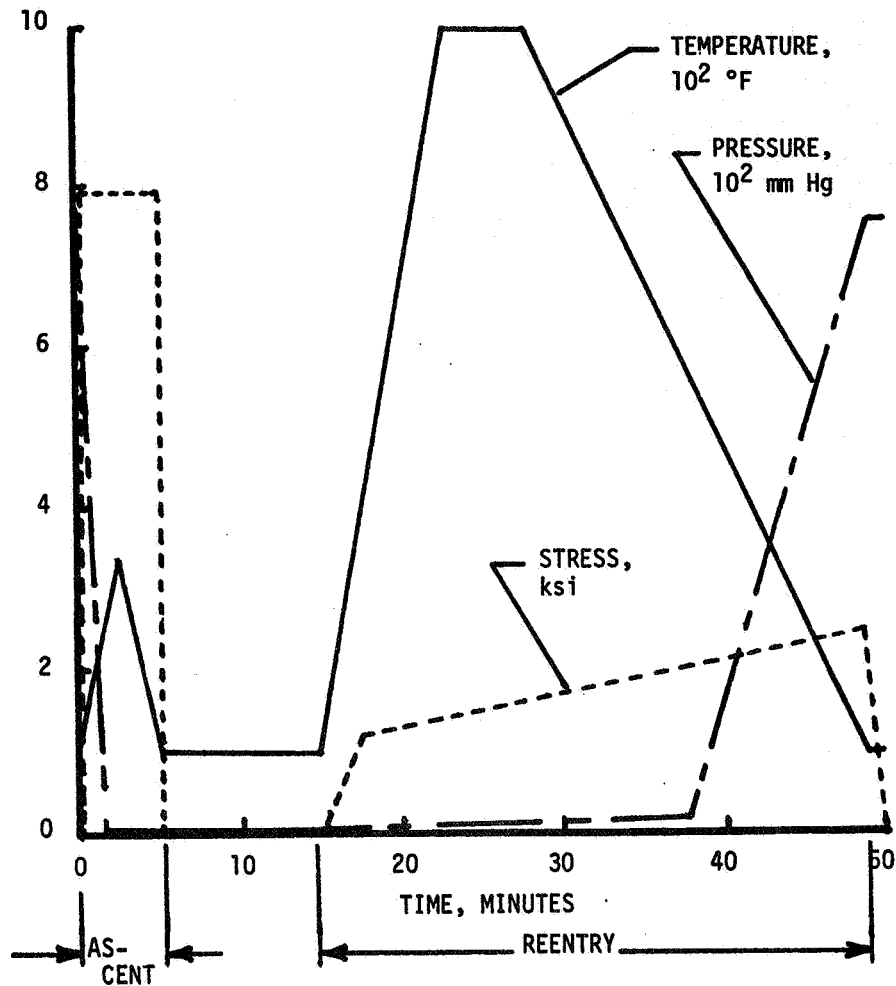


Figure 3- Temperature, pressure, and stress histories for simulated STS exposure of Ti-6Al-4V.

oxidation temperature. Reference 9 gives the following empirical equation for the simultaneous formation of oxide and oxygen solid solution:

$$k = 1.007 \times 10^{-6} \exp(-25400/RT) + 320 \exp(-61800/RT)$$

where k is the overall parabolic constant with units of $\text{gm}^2 \text{cm}^{-4} \text{sec}^{-1}$, R is the gas constant with units of calories/mole °K, and T is the temperature in °K. The units for activation energy are calories/mole. The first exponential is related to oxygen transfer to the substrate. Therefore, the product kt is useful in comparing various exposures or estimating equivalent exposures. It is estimated that one simulated STS mission with a peak temperature of 1000°F, 1100°F, or 1200°F is equivalent to static exposure at the same peak temperature for 7.65, 7.53, or 7.24 minutes, respectively. The static oxidation tests were conducted using these times.

Mechanical Testing Procedure

Tensile tests of foil and sheet specimens were conducted according to the recommended practices of the ASTM (refs. 14 and 15) except that the gage length of the specimen was 1-1/2 in. (fig. 1(b)). Strain of the specimen during loading was determined from two 1-in. gage-length extensometers mounted on opposite faces of the specimen. Yield strength was determined by the 0.2% offset method. The elastic modulus was determined from a least squares fit of a first order equation to the stress-strain data over the stress range of 10 to 60 ksi. Tensile elongation was determined by two methods. One method consists of determining the change in spacing of fiducial marks lightly scribed on the specimen before testing. Pencil marks are placed at 1/4-in. intervals along the gage length of the specimen. At failure, elongation is measured over a 1-in. distance which is centered around the fracture. The second method consists of noting the strain indicated by the extensometers at failure. This last method is valid only when fracture occurs within the gage length of the extensometers.

Results and Discussion

Tables III and IV give results from room temperature tensile tests of Ti-6Al-4V foil and sheet specimens. Data are shown for individual specimens and an average is shown for specimens of each exposure condition. The data show that there was no clear difference in residual mechanical properties of specimens exposed to cyclic conditions (STS 1000 and STS 1100) with and without load; therefore, the loaded and unloaded specimens at each condition are averaged as a single group.

Comparison of Sheet and Foil Data

Figures 4 and 5 show a comparison of the room temperature residual mechanical properties of Ti-6Al-4V sheet and foil in the mill annealed condition, after LID exposure, and after STS 1000 exposure. The ultimate tensile strength of the sheet and foil after LID and STS 1000 exposures was 5% less than the strength in the annealed condition. The yield strength of the foil after LID and STS 1000 exposures was 6% greater than the strength in the annealed condition. However, the yield strength of the sheet after LID and STS 1000 exposures was 8% lower than for the annealed condition.

The tensile moduli of the sheet and foil (fig. 5) were 6% greater after LID and STS 1000 exposures than the modulus in the annealed condition. The tensile elongation of sheet and foil were 20 to 40% greater after LID exposure than in the annealed condition. The tensile elongation of the foil after STS 1000 exposure was less than after LID exposure. The mechanical properties of foil will be discussed further in a later section of this paper.

Figure 6 shows the microstructure of foil and sheet samples in the mill annealed condition, in the LID condition and after STS 1000 exposures. The structure consists of alpha phase with intergranular beta phase. Note the much finer and more elongated grains in the severely worked foil in the mill annealed condition compared to the sheet in the mill annealed condition. The LID process heat treatment increased the grain size of both the sheet and foil, producing equiaxed grains of alpha with intergranular beta. The grain size of the sheet and foil in the LID process condition are about equal. The microstructure of the sheet and foil after STS 1000 exposure consists of equiaxed grains of alpha with intergranular beta. There

Table III.- Residual Room Temperature Mechanical Properties of 0.003 Inch Thick Ti-6Al-4V

Specimen number	Test type	Exposure conditions			Tensile strength		Elastic modulus	Tensile elongation, %	
		Static			Ultimate	Yield		Extensometer	Fiducial marks
		Temp.	Press.	Time	ksi	ksi	Msi		
		°F	mm Hg	hr.					
F-6	Mill annealed*				167.9	132.5	14.1	8.9	10.5
F-7	Mill annealed				169.6	132.6	14.3	10.6	10.0
F-8	Mill annealed				164.6	-	-	-	10.0
F-9	Mill annealed				167.2	131.5	14.1	8.4	10.0
AVG	Mill annealed				167.3	132.2	14.2	9.3	10.1
F-39	LID**				156.7	138.6	14.9	10.9	12.3
F-78	LID				156.2	139.2	15.2	8.4	13.0
F-79	LID				157.2	137.4	15.1	8.7	11.0
F-81	LID				157.4	138.0	15.0	8.3	-
AVG	LID				156.9	138.3	15.1	9.1	12.1
F-83	STS	1000			160.3	141.1	15.3	10.0	9.5
F-89	STS	1000			159.4	142.0	15.2	10.8	10.5
F-84	STS, no stress	1000			160.7	141.8	15.4	10.4	9.2
F-90	STS, no stress	1000			160.3	141.4	15.5	7.5	8.3
AVG	STS	1000			160.2	141.6	15.4	9.7	9.4
F-92	STS	1100			156.5	139.4	15.4	9.0	8.0
F-94	STS	1100			-	-	15.6	-	7.8
F-91	STS, no stress	1100			157.8	140.9	15.5	7.8	7.5
F-93	STS, no stress	1100			156.0	139.0	15.6	-	7.7
AVG	STS	1100			156.8	139.8	15.3	8.4	7.8
F-35A	Static	981	760	12.75	-	-	-	11.5	11.3
F-38A	Static	981	760	12.75	162.3	144.8	15.3	12.3	11.0
F-31A	Static	981	760	12.75	163.2	146.3	15.6	11.1	11.0
AVG	Static	981	760	12.75	162.8	145.6	15.4	11.6	11.1
F-36A	Static	1036	760	12.58	161.3	145.5	15.3	10.8	10.5
F-38B	Static	1036	760	12.58	160.5	147.1	15.5	10.4	10.0
F-37A	Static	1036	760	12.58	160.3	144.0	15.3	10.8	10.0
AVG	Static	1036	760	12.58	160.7	145.5	15.4	10.7	10.2
F-37B	Static	1076	760	12.41	160.1	145.5	15.3	7.3	6.8
F-30A	Static	1076	760	12.41	161.3	145.9	15.3	9.9	9.2
F-34A	Static	1076	760	12.41	161.0	145.5	15.3	10.4	10.0
AVG	Static	1076	760	12.41	160.8	145.6	15.3	9.2	8.7
F-24***	Static	1100	7	12.41	-	145.0	15.6	-	-
F-80***	Static	1100	7	12.41	-	145.0	15.6	-	-
F-85***	Static	1100	7	12.41	-	141.5	15.3	-	-
AVG	Static	1100	7	12.41	-	143.8	15.5	-	-
F-30	Static	1103	760	12.41	160.5	145.1	15.3	9.0	8.0
F-32	Static	1103	760	12.41	160.8	146.7	15.5	9.2	8.2
AVG	Static	1103	760	12.41	160.7	145.9	15.4	9.1	8.1
F-35B	Static	1123	760	12.24	161.8	147.8	15.6	-	7.0
F-34B	Static	1123	760	12.24	160.6	145.5	15.4	7.3	6.0
F-33A	Static	1123	760	12.24	158.6	143.6	15.5	9.0	8.0
AVG	Static	1123	760	12.24	160.3	145.6	15.5	8.0	7.0
F-33B	Static	1177	760	12.07	154.6	141.7	15.9	4.7	4.0
F-32A	Static	1177	760	12.07	154.0	142.5	15.8	4.4	3.3
F-36B	Static	1177	760	12.07	154.0	141.7	15.9	-	3.5
AVG	Static	1177	760	12.07	154.2	142.0	15.9	4.5	3.6
F-86	Static	1200	7	12.07	145.4	138.8	15.9	2.7	3.0
F-88	Static	1200	7	12.07	145.9	140.1	16.0	1.8	3.5
AVG	Static	1200	7	12.07	145.6	139.5	15.9	2.3	3.3

*Specimens from as-received materials are referred to as mill annealed.

**Specimens exposed to oxidation conditions received LID process heat treatment before exposure.

***This series of specimens failed outside region of indicated exposure conditions.

Table IV.- Residual Room Temperature Mechanical Properties
of 0.035 Inch Thick Ti-6Al-4V

Specimen number	Test type	Exposure temperature	Tensile strength		Elastic modulus	Tensile elongation,
			Ultimate	Yield		%
		°F	ksi	ksi	Msi	Fiducial marks
S-57	Mill annealed*		155.3	147.5	16.5	13.0
S-58	Mill annealed		151.4	142.7	15.9	14.0
S-59	Mill annealed		155.3	148.1	16.1	12.0
AVG	Mill annealed		154.0	146.1	16.2	13.0
S-27	LID**		146.4	131.9	17.0	17.0
S-28	LID		146.0	132.0	16.9	18.0
S-29	LID		145.3	132.5	17.0	18.0
AVG	LID		145.9	134.1	16.9	17.7
S-21***	STS	1000	-	135.5	17.0	-
S-23***	STS	1000	-	136.8	17.0	-
S-22***	STS, no stress	1000	-	136.1	17.0	-
S-24***	STS, no stress	1000	-	136.8	17.1	-
AVG	STS	1000	-	136.3	17.0	-

*Specimens from as-received material are referred to as mill annealed.

**Specimens exposed to STS conditions received LID process heat treatment.

***Failure occurred outside zone of indicated exposure conditions.

appears to be substantially less beta phase after STS 1000 exposure than after LID exposure.

The LID process heat treatment to which sheet and foil specimens were exposed represents an anneal just below the beta transus with a furnace cool. The sheet and foil microstructures, consisting of equiaxed alpha grains with intergranular beta (fig. 6), which formed during that heat treatment resulted in the loss in strength and gain in ductility from mill annealed to LID (figs. 4 and 5). The increase in modulus from mill annealed to LID (fig. 5) is a result of the increase in the alpha- to beta-phase ratio (ref. 16).

The simulated TPS exposures utilized in the present study are analogous to aging heat treatments. However, the microstructural changes and the oxidation/contamination of the alloy are competing mechanisms in terms of their effect on mechanical properties. The lesser presence of beta phase in the STS-exposed sheet and foil (fig. 6), compared to the LID exposed sheet and foil, resulted from transformation of the beta phase to the more stable alpha phase.

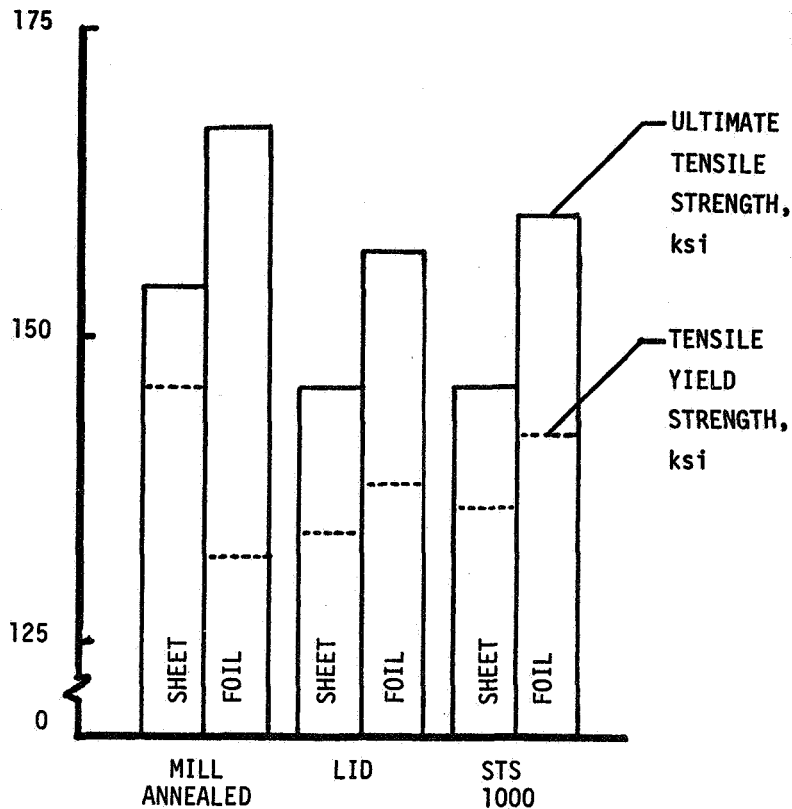


Figure 4- Comparison of room temperature tensile strength of Ti-6Al-4V sheet and foil (data are average of four specimens each).

Foil Mechanical Properties

Figures 7-10 show residual room temperature ultimate tensile strength, tensile yield strength, elastic modulus, and tensile elongation of foil gage Ti-6Al-4V in the mill annealed condition, after LID process heat treatment, and after exposure to static oxidation and cyclic oxidation (STS 1000 and STS 1100) conditions. The ultimate tensile strength (fig. 7) of foil after oxidation at temperatures from 980°F to 1125°F is greater than the tensile strength of foil after LID exposure (see Table III). Foil oxidized at temperatures higher than 1125°F suffered a loss in tensile strength. The strengths of the STS 1100 specimens are about 2% lower than the strengths of the specimens statically oxidized at 1100°F.

The yield strength (fig. 8) of oxidized foil specimens is greater than the yield strength of the mill annealed and LID exposed specimens. Yield strength of statically oxidized specimens is constant with oxidation temperatures from 980° to 1125°F. At oxidation temperatures greater than 1125°F the yield strength decreases. The yield strength of the STS-exposed specimens is about 3% lower than the yield strength of comparably static-oxidized specimens.

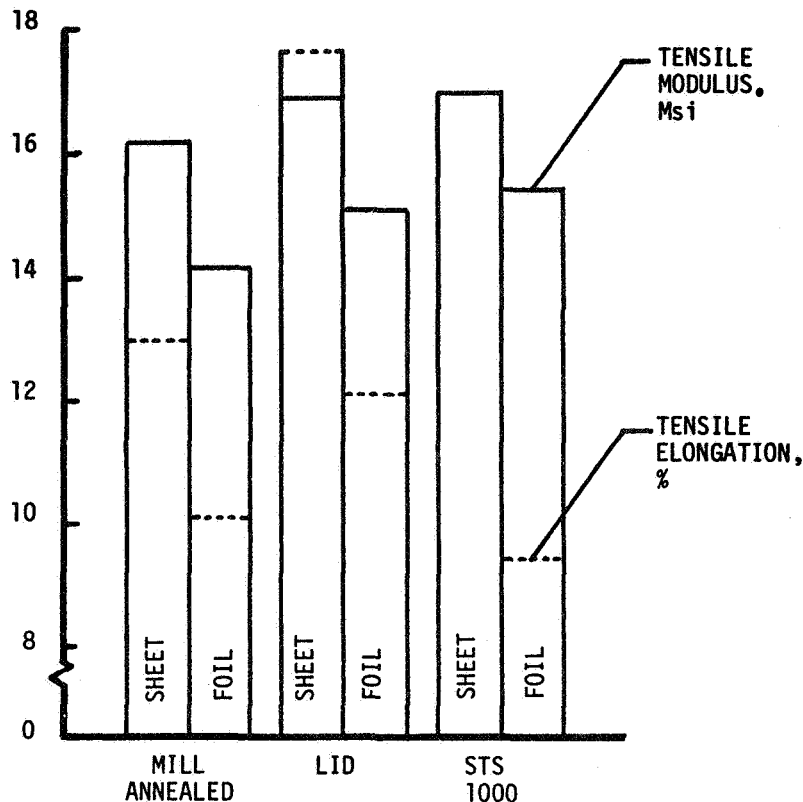


Figure 5- Comparison of room temperature tensile modulus and elongation of Ti-6Al-4V sheet and foil (data are average of four specimens each).

The elastic modulus (fig. 9) of oxidized foil specimens is greater than the elastic modulus of LID exposed specimens. The modulus is constant with oxidation temperature to 1125°F. At oxidation temperatures above 1125°F the modulus increases with temperature. The increase in modulus with exposure temperature results from the increase in the alpha- to beta-phase ratio at higher aging temperatures (ref. 16).

Figure 10 shows Ti-6Al-4V foil specimen tensile elongation data for a 1-in. section about the fracture zone. Two sources of data are indicated - the open symbols represent data from fiducial marks on the specimen and the closed symbols represent data from the extensometers attached to the specimen. Extensometer data are shown only for those cases where fracture of the specimen occurred within the gage length of the extensometer. The extensometer data are consistently higher than the fiducial mark data because the extensometer output includes elastic strain and plastic strain; agreement between the two methods is good. The elongation of the oxidized specimens was less than the elongation of the LID exposed specimens. The data for the statically oxidized specimens decreases linearly with oxidation temperature to 1125°F. The elongation drops more rapidly with increases in temperature above 1125°F. The elongation of STS-exposed specimens is slightly lower than that for statically oxidized specimens.

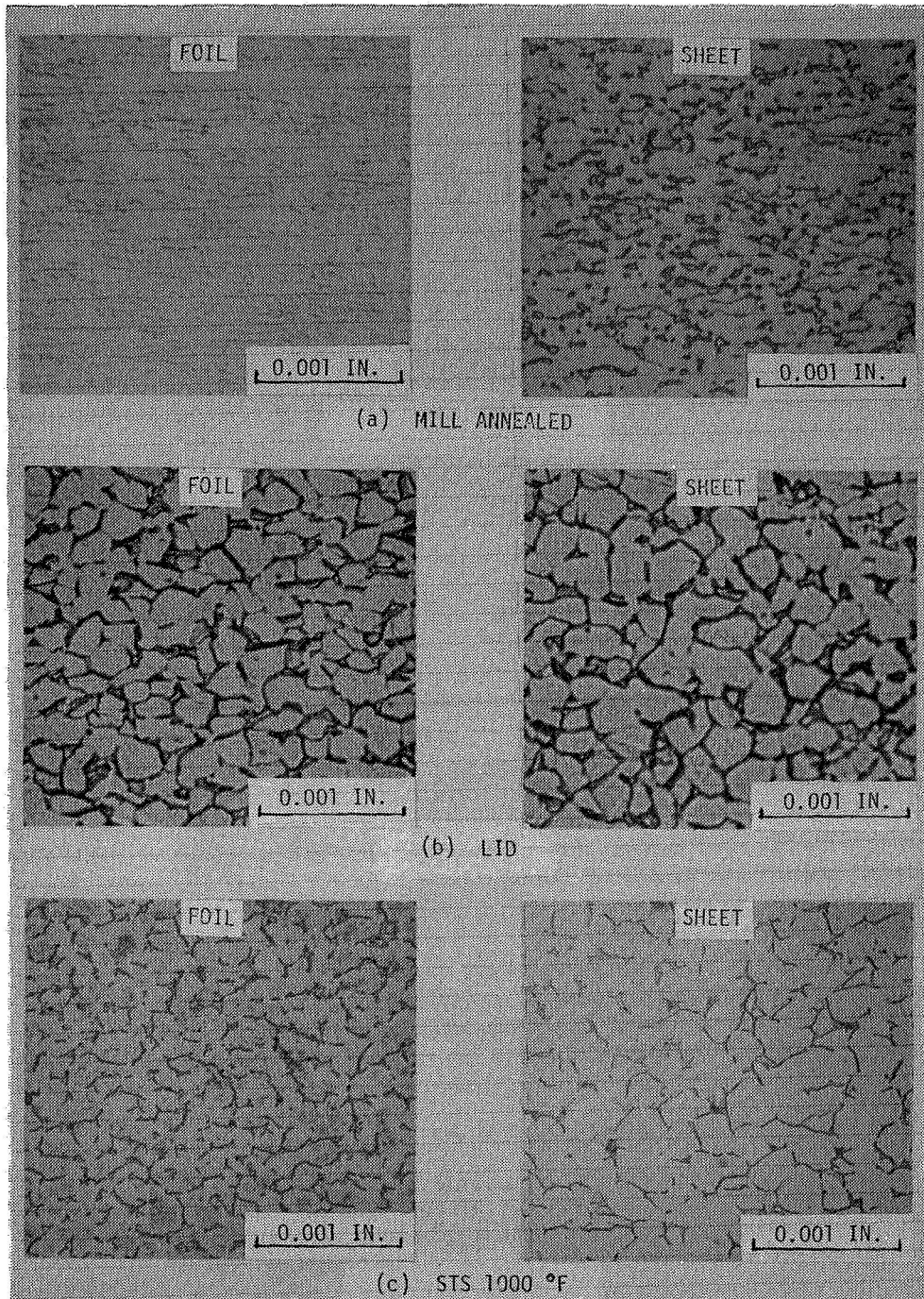


Figure 6- Microstructure of Ti-6Al-4V sheet and foil in the mill annealed condition, after LID heat treatment, and after STS 1000 exposure.

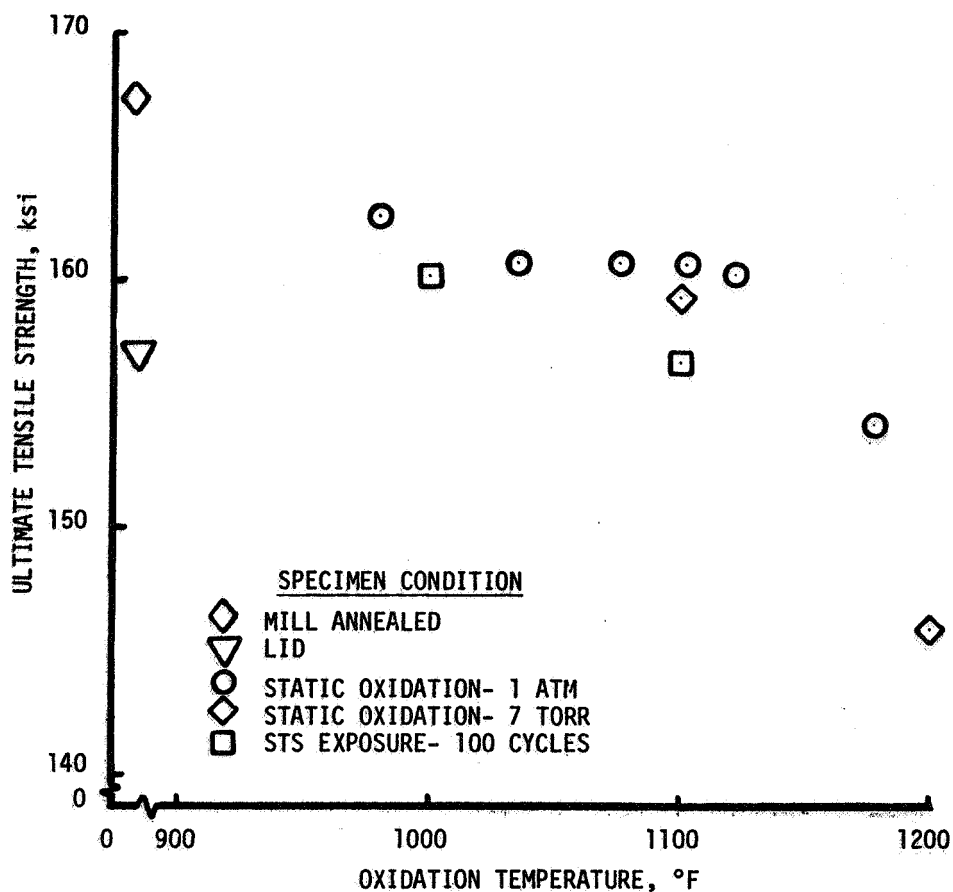


Figure 7- Effect of oxidation temperature on average room temperature ultimate tensile strength of Ti-6Al-4V foil.

The data in figures 7-10 do not show a significant difference between the residual mechanical properties of specimens statically oxidized at a pressure of 1 atm and at a pressure of 7 torr.

Foil Microstructures and Oxidation/Embrittlement Mechanisms

Figure 11 shows a comparison of the microstructure of Ti-6Al-4V foil after STS 1000 and STS 1100 exposures with and without stress. Each microstructure shown here consists of equiaxed grains of alpha with intergranular beta. No effect of stress is notable in the microstructures.

Figure 12 shows a comparison of the microstructure of Ti-6Al-4V foil after STS 1100 exposure and after static oxidation at 1100°F for an equivalent time. There are no significant differences in microstructure of the STS-exposed and static-exposed specimens.

The thickness of oxide scale formed during static and STS exposures of specimens, which was determined to be much less than 1.0 μm for all

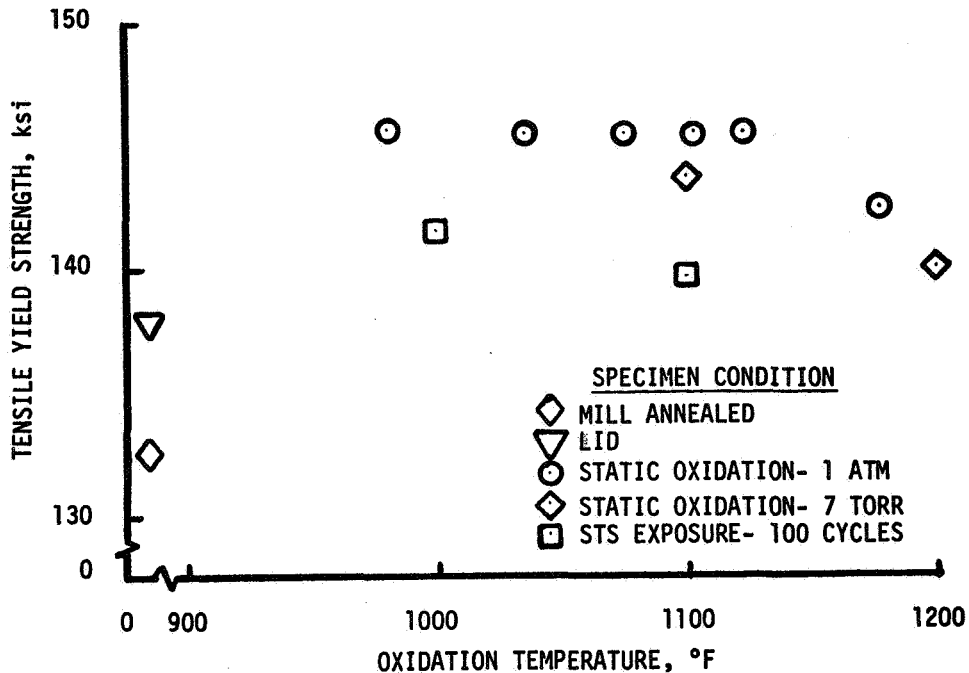


Figure 8- Effect of oxidation temperature on average room temperature tensile yield strength of Ti-6Al-4V foil.

exposure conditions, does not represent a significant loss in material thickness. However, diffusion of oxygen into the alloy where it exists as interstitial atoms in solid solution is a significant event. The microhardness of the alloy increases as the level of oxygen in solution increases (refs. 7 and 8). Figure 13 shows microhardness profiles for specimens after STS 1000 and STS 1100 exposures. The hardness measurements were made with a Knoop diamond indenter using a 1-gram weight. The data show that the total contamination depth is about 19 μm and the contamination depth for a microhardness increase of 40 KHN is about 10 μm for both exposure conditions. Reference 8 shows that cracking of the alpha case of tensile loaded, oxygen contaminated titanium specimens occurs to a depth of 40 KHN hardness increase

Figure 14 shows photomicrographs of the cross section of specimens tested to failure in tension after static and STS exposures at 1000° and 1100°F. Note the presence of cracks at the surface. The depth of cracks is much greater at 1100°F than at 1000°F for both the static- and STS-exposed specimens. Also note that the crack density in the STS specimens is greater than in the static specimens for 1000° and 1100°F exposures. The surface cracks shown in figure 14 are the result of failure of the case-hardened layer during tensile loading. Cracks in the surface act as stress risers and result in premature failure of specimens.

Reference 17 presents data which show that removal of the case-hardened layer from oxygen contaminated titanium specimens restores the mechanical properties, including tensile elongation, to their initial values.

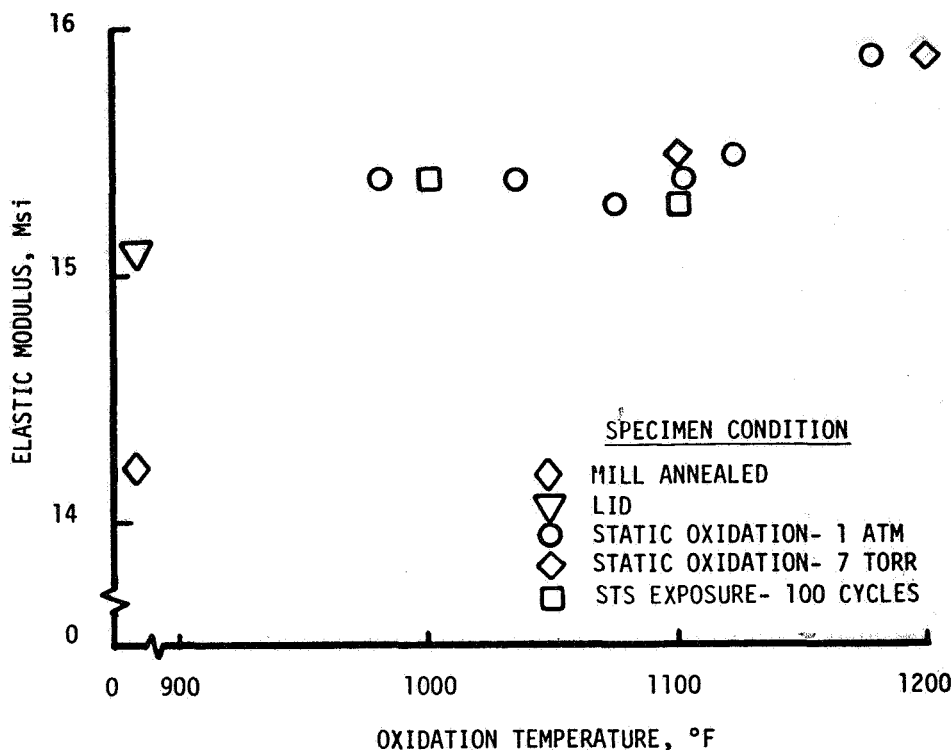


Figure 9- Effect of oxidation temperature on average room temperature elastic modulus of Ti-6Al-4V foil.

That fact demonstrates that embrittlement of titanium is a surface phenomenon. Because embrittlement is a surface phenomenon and its effect is related to the surface to volume ratio, titanium in sheet form would not be significantly affected by exposure to temperatures to 1200°F for 12 hours.

All of the phenomena whereby titanium becomes embrittled on absorbing oxygen are not understood; however, oxygen is known to shift the solubility limit of aluminum in alpha-phase titanium to lower values, thereby increasing the likelihood of Ti_3Al formation (ref. 16). Ti_3Al precipitates together with absorbed oxygen alter the alpha-phase deformation characteristics and thus influence the mechanical properties of the alloy (ref. 14); however, TEM examination of a 1200°F statically oxidized specimen showed no evidence of Ti_3Al precipitates.

The small difference in mechanical properties of static versus cyclic (STS) oxidation specimens which is most evident in the residual strength data (ultimate tensile strength and tensile yield strength, figs. 7 and 8) and in the depth of cracks in the alpha case (fig. 14) was examined further by exposing twelve weight-gain specimens each to cyclic oxidation with a peak temperature of 1300°F and static oxidation at a temperature of 1300°F. The cyclic exposures spanned 28 cycles of rapid heat-up and cool-down with a 6-minute hold at 1300°F. The static exposures were for 3 hours and 13 minutes which is the time equivalence of cyclic exposures from kinetic

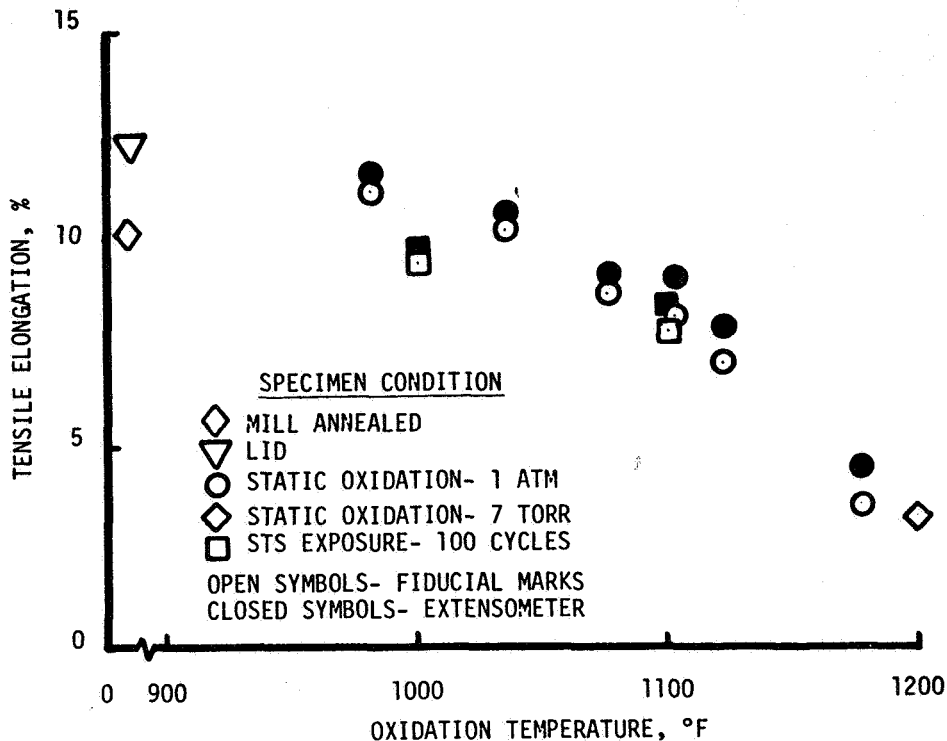


Figure 10- Effect of oxidation temperature on average room temperature tensile elongation (1-inch gage length) of Ti-6Al-4V foil.

considerations. The specimens exposed to cyclic conditions experienced a 10% greater increase in mass than did the specimens exposed to static conditions. However, though a greater oxygen pickup by the cyclic specimens is consistent with lower strength and more severe cracking of the alpha case, a 10% difference in mass change alone should not produce a noticeable difference in mechanical performance. This fact is supported by the data in figure 8 where the tensile yield strength of the statically oxidized specimens is constant with oxidation temperature over the temperature range from 980° to 1125°F even though the mass change over that temperature range differs by a factor of 3 to 5. Based on these factors, it is likely that the small differences in mechanical properties of static versus cyclic oxidation specimens results for a combination of factors including microstructure differences, oxide thickness differences, and oxygen contamination differences.

Conclusions

Microstructure and mechanical properties were determined to Ti-6Al-4V in sheet and foil thicknesses after exposure to simulated STS ascent-reentry conditions at peak temperatures ranging from 1000°F to 1200°F. Results from those tests and other cognizant results in the literature support the following conclusions:

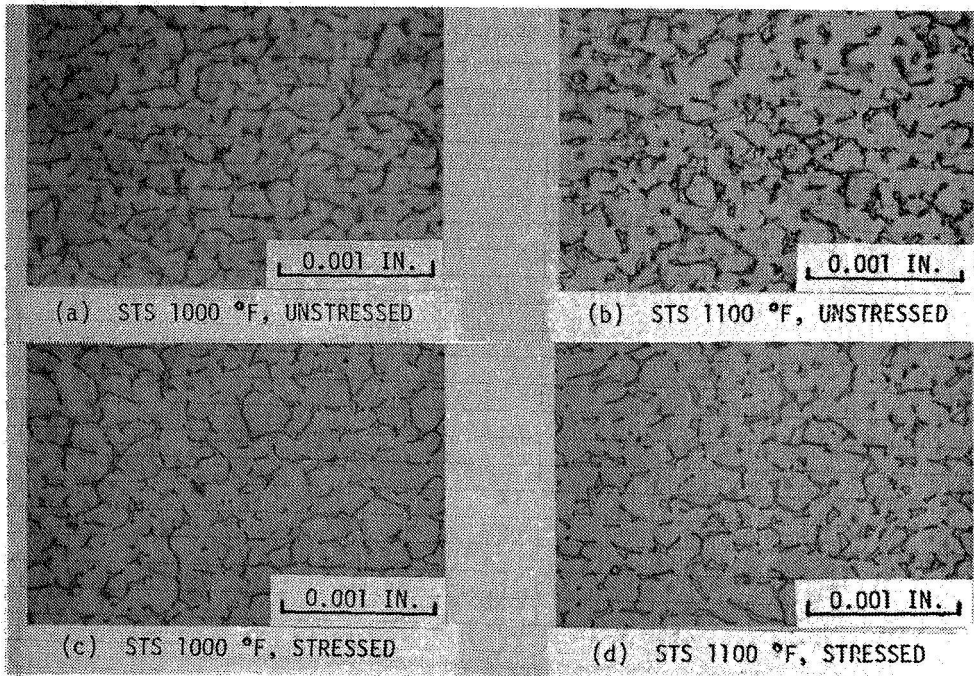


Figure 11- Comparison of microstructure of Ti-6Al-4V foil after STS 1000 and STS 1100 exposures.

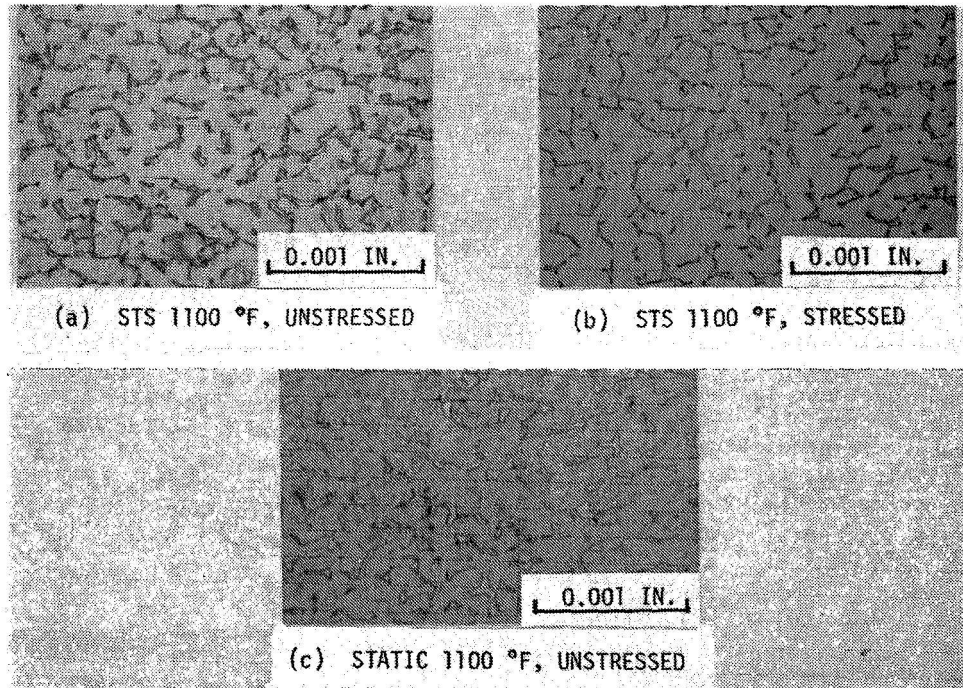


Figure 12- Comparison of microstructure of Ti-6Al-4V foil after static oxidation at 1100 °F and after STS exposure at 1100 °F with and without stress.

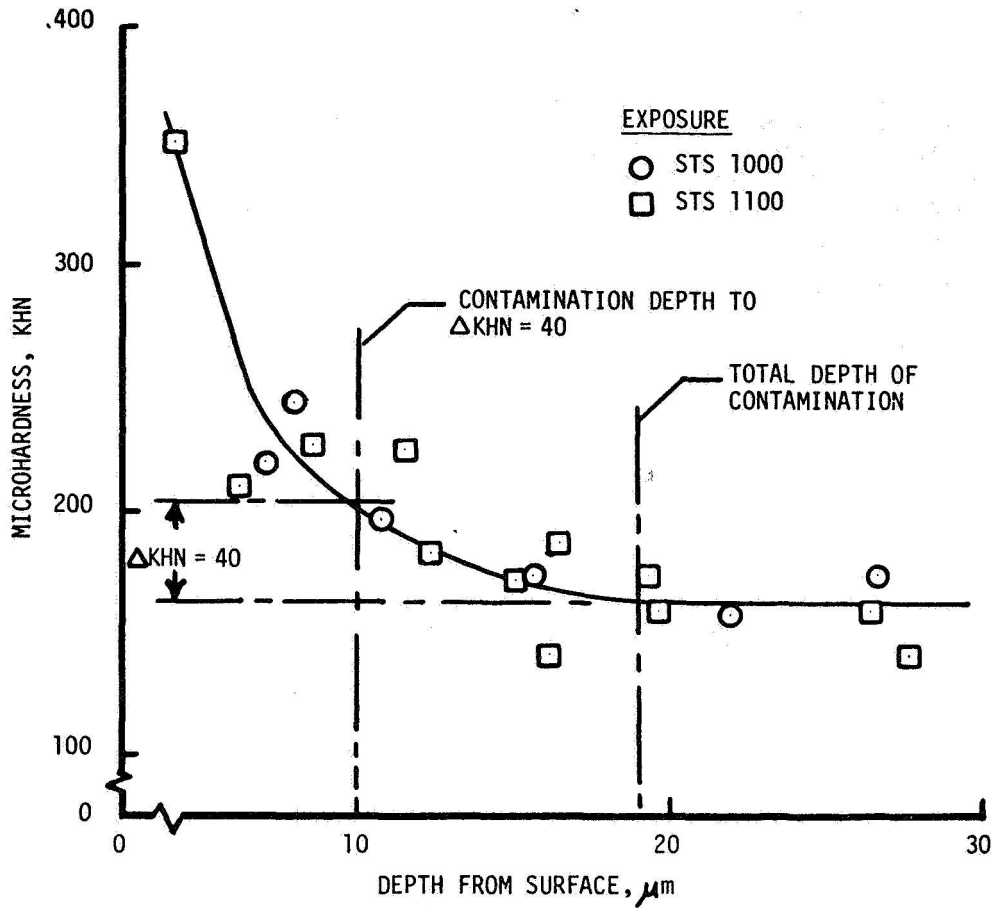


Figure 13- Microhardness profiles for Ti-6Al-4V foil after STS 1000 and STS 1100 exposures.

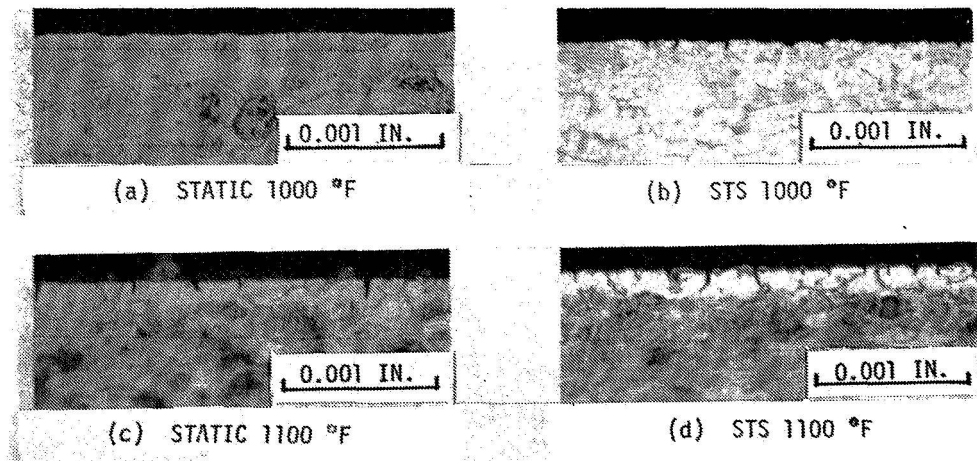


Figure 14- Cross-section photomicrographs of Ti-6Al-4V after tensile testing showing presence of cracks at the surface.

1. Mechanical design properties (tensile strengths and moduli) of Ti-6Al-4V foil are not significantly affected by simulated TPS service conditions.

2. The mechanical property of Ti-6Al-4V that is most sensitive to the simulated TPS service environment is tensile elongation. The residual tensile elongation of specimens after exposure to 100 simulated ascent-reentry missions with a peak temperature of 1100°F is about 8% compared to 12% for specimens annealed to below the beta transus and 3% for specimens after ascent-reentry with a peak temperature of 1200°F.

3. The principal cause of loss in tensile elongation of Ti-6Al-4V with exposure to TPS service conditions is oxygen contamination. Oxygen contamination results from diffusion of oxygen into the alloy. The affected region forms an embrittled layer at the surface which develops cracks under tensile load and fails prematurely. The contamination depth (to $\Delta KHN = 40$) resulting from 100 missions of simulated reentry at 1100°F is about 10 μm .

4. Titanium oxide (TiO_2) formed on Ti-6Al-4V during exposure to 100 missions of simulated reentry at temperatures to 1200°F does not represent a major loss in material thickness even for foil gage material.

5. The microstructure of Ti-6Al-4V sheet and foil in the LID processed conditions is equiaxed alpha grains with intergranular beta phase. Significant beta-to-alpha transformation appears to take place with exposure to simulated TPS conditions.

6. Stress as a parameter during the STS exposures of sheet and foil specimens did not have a discernible affect on the residual mechanical properties.

7. Specimens exposed to STS (cyclic) oxidation had 2 to 3% lower strength and more severe cracking of the alpha case than did the specimens exposed to static oxidation. These small differences probably result from a combination of factors including differences in microstructure, oxide thickness, and oxygen contamination.

References

1. Robert L. Jackson and Sidney C. Dixon, "A Design Assessment of Multiwall, Metallic Stand-Off, and RSI Reusable Thermal Protection Systems Including Space Shuttle Application," NASA TM-8170, April 1980.
2. Allan H. Taylor and Robert L. Jackson, "Thermo-Structural Analyses of Structural Concepts for Hypersonic Cruise Vehicles," AIAA Paper No. 80-0407, Pasadena, CA, Jan. 1980.
3. Angelo Varisco, Paul Bell, and Willie Wolter, "Design and Fabrication of Metallic Thermal Protection Systems for Aerospace Vehicles," NASA CR-145313, Feb. 1978.
4. R. J. McClintick, G. W. Bauer, and L. S. Busch, "Physical Metallurgy and Heat Treatment of Titanium Alloys." Mallory-Sharon Titanium Corp., 1955.
5. S. R. Seagle and L. J. Bartlo, "Physical Metallurgy and Metallography of Titanium Alloys," Metals Engineering Quarterly, Vol. 8, Aug. 1968.

6. Matthew J. Donachie, Jr., ed., "Titanium and Titanium Alloys," American Society for Metals, 1982.
7. Jalaiah Unnam, R. N. Shenoy, and Ronald K. Clark, "Effect of Alloy Chemistry and Exposure Conditions on the Oxidation of Titanium," TMS-AIME Paper No. A84-57, 1984 TMS-AIME Annual Meeting, Los Angeles, CA, Feb. 1984.
8. C. E. Shamblen and T. K. Redden, "Air Contamination and Embrittlement of Titanium Alloys," Proceedings International Conference on Titanium, Institute of Metals, Metallurgical Society AIME, and American Society for Metals, London, England, May 21-24, 1968.
9. J. Stringer, "The Oxidation of Titanium in Oxygen at High Temperatures," Acta Metallurgical, Vol. 8, Nov. 1960.
10. W. Blair, J. E. Meaney, Jr., and H. A. Rosenthal, "Design and Fabrication of Titanium Multiwall Thermal Protection System (TPS) Test Panels," NASA CR-159241, 1980.
11. W. Blair, J. E. Meaney, Jr., and H. A. Rosenthal, "Fabrication of Titanium Multiwall Thermal Protection Systems (TPS) Test Panel Arrays," NASA CR-159383, 1980.
12. Don E. Avery, John L. Shideler, and Robert N. Stuckey, "Thermal and Aerothermal Performance of a Titanium Multiwall Thermal Protection System," NASA TP-1961, Dec. 1981.
13. C. W. Stroud and Donald R. Rummler, "Mass Loss of a TEOS-Coated, Reinforced Carbon-Carbon Composite Subjected to a Simulated Shuttle Entry Environment," NASA TM-81799, July 1980.
14. E 345-81, "Standard Methods of Tension Testing of Metallic Foil," 1982 Annual Book of ASTM Standards, Part 10.
15. E 8-81, "Standard Methods of Tension Testing of Metallic Materials," 1982 Annual Book of ASTM Standards, Part 10.
16. Gerhard Welsch and Wolfgang Bunk, "Deformation Modes of the α -Phase of Ti-6Al-4V as a Function of Oxygen Concentration and Aging Temperature." Metallurgical Transactions A, Vol. 13A, May 1982.
17. L. A. Glikman, V. I. Deryabina, N. N. Kolgatin, I. A. Bytenskii, V. P., Teodorovich, and N. S. Teplov, "The Influence of Gas-Saturated Layers on the Strength and Plastic Properties of Titanium Alloys." "Titanium and Its Alloys," I. I. Kornilov, ed., NASA TT F-362, 1966.

1. Report No. NASA TM-86294		2. Government Accession No.		3. Recipient's Catalog No.	
4. Title and Subtitle Residual Mechanical Properties of Ti-6Al-4V After Simulated Space Shuttle Reentry				5. Report Date August 1984	
				6. Performing Organization Code 506-53-33-01	
7. Author(s) Ronald K. Clark Jalaiah Unnam				8. Performing Organization Report No.	
				10. Work Unit No.	
9. Performing Organization Name and Address NASA Langley Research Center Hampton, VA 23665				11. Contract or Grant No.	
				13. Type of Report and Period Covered Technical Memorandum	
12. Sponsoring Agency Name and Address National Aeronautics and Space Administration Washington, DC 20546				14. Sponsoring Agency Code	
15. Supplementary Notes R. K. Clark, NASA Langley Research Center, Hampton, VA; J. Unnam, Analytical Service and Materials, Inc., Tabb, VA This paper, available as TMS-AIME Paper No. A84-57, was presented at the 1984 Annual Meeting of TMS-AIME in Los Angeles, CA, February 28-March 2, 1984					
16. Abstract Oxidation and embrittlement are concerns in use of titanium foils for shielding advanced space transportation system vehicles during Earth reentry. Ti-6Al-4V in 0.003 in. and 0.035 in. thicknesses were exposed to multiple cycles of simulated space transportation system ascent-reentry conditions at temperatures ranging from 1000°F to 1200°F. Residual mechanical tests and metallurgical analyses were made on the specimens after exposure. Results show that tensile elongation is the mechanical property most affected by the reentry environment. Results are presented to show a comparison of residual properties of foil specimens from static oxidation exposure and cyclic oxidation exposure.					
17. Key Words (Suggested by Author(s)) Titanium Oxidation Titanium Mechanical Properties Heat Shields			18. Distribution Statement Unclassified-Unlimited Subject Category 26		
19. Security Classif. (of this report) Unclassified	20. Security Classif. (of this page) Unclassified	21. No. of Pages 22	22. Price* A02		